Received: 11 September 2020 | Revised: 4 November 2020 | Accepted: 28 December 2020

DOI: 10.1111/pce.13990

ORIGINAL ARTICLE

Plant, Cell & Environment WILEY

Photosystem II heat tolerances characterize thermal generalists and the upper limit of carbon assimilation

Timothy M. Perez[1] | Annika Socha[2] | Olga Tserej[3,4] | Kenneth J. Feeley[3,4]

[1]Department of Botany and Biodiversity Research Centre, University of British Columbia, Vancouver, British Columbia, Canada

[2]Nicholas School of the Environment, Duke University, Durham, North Carolina

[3]Department of Biology, University of Miami, Coral Gables, Florida

[4]Fairchild Tropical Botanic Garden, Coral Gables, Florida

Correspondence
Timothy M. Perez, Department of Botany and Biodiversity Research Centre, University of British Columbia, Vancouver, BC V6T 1Z4, Canada.

Funding information
Garden Club of America, Grant/Award Number: Award in Tropical Botany; National Science Foundation, Grant/Award Number: DEB-1350125

Abstract

The heat tolerance of photosystem II (PSII) may promote carbon assimilation at higher temperatures and help explain plant responses to climate change. Higher PSII heat tolerance could lead to (a) increases in the high-temperature compensation point (T_{max}); (b) increases in the thermal breadth of photosynthesis (i.e. the photosynthetic parameter Ω) to promote a thermal generalist strategy of carbon assimilation; (c) increases in the optimum rate of carbon assimilation P_{opt} and faster carbon assimilation and/or (d) increases in the optimum temperature for photosynthesis (T_{opt}). To address these hypotheses, we tested if the T_{crit}, T_{50} and T_{95} PSII heat tolerances were correlated with carbon assimilation parameters for 21 plant species. Our results did not support Hypothesis 1, but we observed that T_{50} may be used to estimate the upper thermal limit for T_{max} at the species level, and that community mean T_{crit} may be useful for approximating T_{max}. The T_{50} and T_{95} heat tolerance metrics were positively correlated with Ω in support of Hypothesis 2. We found no support for Hypotheses 3 or 4. Our study shows that high PSII heat tolerance is unlikely to improve carbon assimilation at higher temperatures but may characterize thermal generalists with slow resource acquisition strategies.

KEYWORDS
carbon reactions, climate change, electron transport, leaf economics spectrum, mountain passes hypothesis, photosynthetic temperature response

1 | INTRODUCTION

The heat tolerance of plants' photosystem II (PSII) photochemistry may provide a useful estimate of the upper thermal limit of photosynthesis and has the potential to explain the physiological mechanisms underlying some of the ecological responses of plants to climate change (Clark, Piper, Keeling, & Clark, 2003; Doughty & Goulden, 2009; Feeley, Bravo-Avila, Fadrique, Perez, & Zuleta, 2020; Mau, Reed, Wood, & Cavaleri, 2018; Pau, Detto, Kim, & Still, 2018). Higher heat tolerance of PSII photochemistry is generally assumed to allow for improved growth, reproduction and/or survival in hot environments, presumably by facilitating photosynthesis at high temperatures (Feeley, Martinez-villa, Perez & Duque 2020; Krause, Winter, Krause, & Virgo, 2015; Tiwari et al., 2020; but see Perez & Feeley, 2020a, 2020b). However, these assumptions have not been widely tested, and it is unclear how PSII heat tolerance integrates with different thermal strategies for understanding the effects of climate change on plants.

Heat tolerance of PSII is commonly measured using chlorophyll *a* fluorescence. Early studies to adopt the use of chlorophyll fluorescence quantified PSII heat tolerance using the F_0 fluorometric parameter, which indicates the number of maximally open reaction centres and found that it was correlated with T_{max}—the temperature at which carbon assimilation approaches zero (Downton, Berry, & Seemann, 1984; Seemann, Berry, & Downton, 1984). However, F_0 can provide biased estimates of PSII function during heat treatments that change leaf optical properties (Baker, 2008), leading many researchers to adopt the maximum quantum yield (F_v/F_m) fluorometric as a more robust metric for estimating PSII heat tolerance where $F_v = F_m - F_0$, and F_m indicates closed reaction centres in saturating light (Baker, 2008; Maxwell & Johnson, 2000).

Although F_v/F_m can reliably measure PSII function under stress treatments and is commonly used to measure PSII heat tolerance, F_v/F_m may not be a reliable proxy for carbon assimilation under field conditions. F_v/F_m is only proportional to carbon assimilation under low light conditions and when photorespiration is minimized (Baker, 2008; Brooks & Farquhar, 1985). These conditions are not met in the field when leaves experience high light and temperatures. It is unclear if F_v/F_m heat tolerance promotes carbon assimilation in hotter environments, but some empirical evidence and ecological theory support this assumption.

As was shown with heat tolerance estimates that used F_0 (Downton et al., 1984; Seemann et al., 1984), one way that high PSII heat tolerance could promote photosynthesis at higher temperatures is if it is correlated with T_{max}. Reported values for T_{max} in tropical plant species range from 40.1 to 41.8°C and are comparable to the temperatures that cause the first signs of damage in F_v/F_m (i.e. T_{crit}) for tropical species (Figure 1a; Perez & Feeley, 2020a; Slot, Krause, Krause, Hernández, & Winter, 2018; Tiwari et al., 2020). Coordination between T_{crit} and T_{max} would provide support for the hypothesis that PSII heat tolerance constrains the upper limit of carbon assimilation by limiting electron transport (Slot & Winter, 2017a).

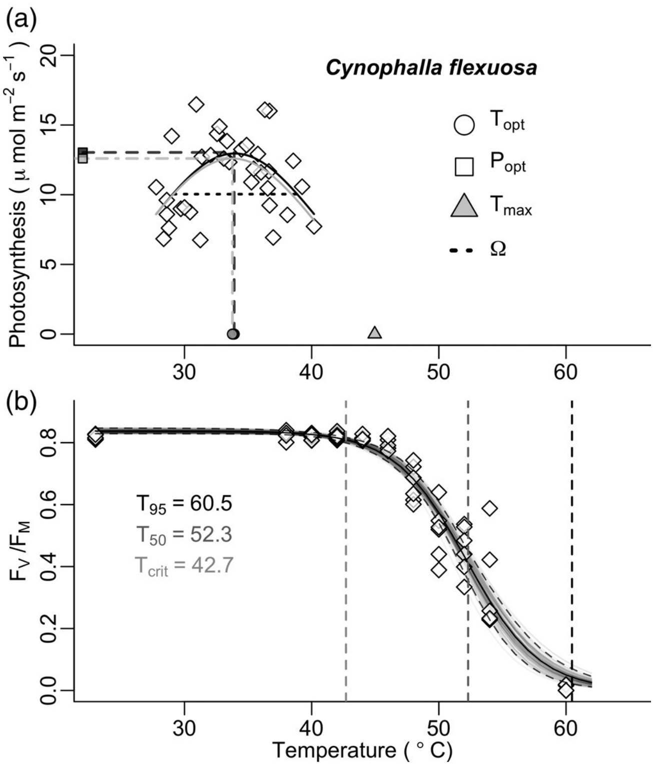

FIGURE 1 (a) Illustrates carbon assimilation as a function of leaf temperature for a single exemplar species, *Cynophalla flexuosa*. The black and grey colours indicate Equations (1) and (2) model fits to the diamond-shaped data points, respectively. Equation (1) was used to calculate T_{opt}, P_{opt} and Ω; Equation (2) was used to calculate T_{opt}, P_{opt} and T_{max}; (b) illustrates the quantum yield (F_v/F_m) as a function of temperature treatment used to calculate the T_{crit}, T_{50} and T_{95} heat tolerance (represented as shaded vertical lines) using Equations (3) and (4) for *C. flexuosa*. The curved shaded lines show 1 of 100 bootstrapped iterations

Another way that PSII heat tolerance could promote carbon assimilation at higher temperatures is by increasing the breadth of temperatures over which carbon assimilation can occur (Ω; Figure 1a; Cunningham & Read, 2003; Slot & Winter, 2017a). The Ω metric can be used to characterize plants as physiological thermal 'generalists' versus 'specialists', which is similar to what has done with animal species (Ghalambor, Huey, Martin, Tewksbury, & Wang, 2006; Huey, 2012; Huey & Hertz, 1984). A positive correlation between PSII heat tolerance and Ω would be consistent with a thermal generalist strategy of carbon assimilation and would provide a physiological explanation for why thermal specialist plant species are more susceptible to climate change than generalist species (Ghalambor et al., 2006; Janzen, 1967; Perez, Stroud, & Feeley, 2016). Indeed, Ω is also a key trait linking leaf thermoregulation to the 'fast–slow' leaf economic spectrum (Michaletz et al., 2015, 2016). Since variation in PSII heat tolerance is driven by high leaf temperatures (Perez & Feeley, 2020a) and 'fast' species are expected to have high leaf temperatures and large Ω (Michaletz et al., 2015, 2016), PSII heat tolerance is expected to be proportional to Ω.

Plants with fast resource acquisition strategies are characterized in part by their high rates of carbon assimilation (Reich, 2014; Wright et al., 2004). The plant economic spectrum typically proposes that fast strategies are characterized by poor physiological tolerances (Reich, 2014), such that the optimum rates of photosynthesis (P_{opt}, Figure 1a) and PSII heat tolerances may be inversely proportional. Conversely, since fast species are also characterized by high leaf temperatures (Michaletz et al., 2015, 2016), PSII heat tolerance may be positively correlated to P_{opt}. This expectation is consistent with the idea that high PSII heat tolerance is beneficial for plants growing in hot environments.

The optimum temperature for carbon assimilation (T_{opt}, Figure 1a) is another important parameter that describes carbon assimilation as a function of temperature and is potentially coordinated with PSII heat tolerance. For example, species tend to increase in both their PSII heat tolerance and T_{opt} when grown in hotter environments (Valladares & Pearcy, 1997; Way & Yamori, 2014; Zhu et al., 2018). High PSII heat tolerance may promote increases in T_{opt} by improving electron transport or the availability of ATP and NADH at high temperatures (Baker, 2008; Genty, Briantais, & Baker, 1989; Maxwell & Johnson, 2000), in support of the assumption that PSII heat tolerance will facilitate carbon assimilation in hot environments.

In this study, we measured three common metrics of PSII heat tolerance that indicate the temperatures that cause an initial, 50 and 95% decrease in F_v/F_m (T_{crit}, T_{50} and T_{95}, respectively; Figure 1b). We compared these metrics of heat tolerance to T_{max}, P_{opt}, T_{opt} and Ω for 21 plant species grown in a quasi 'common garden' environment (Fairchild Tropical Botanic Garden, Coral gables, FL; Perez et al., 2019). We tested four hypotheses consistent with the assumption that high PSII heat tolerance promotes carbon assimilation in hotter environments. Specifically, we looked at the correlations among the different metrics of heat tolerance and carbon assimilation after controlling for any potential effect of phylogenetic non-independence to test the hypotheses that (H1) T_{max} is constrained by PSII heat tolerance; (H2) high PSII heat tolerance is indicative of a thermal generalist strategy of carbon assimilation; (H3) high PSII heat tolerance is characteristic of species with fast carbon acquisition strategies and (H4) high PSII heat tolerance promotes higher T_{opt} (Figure 2).

2 | MATERIALS AND METHODS

2.1 | Site and species selection

This study used plants in the living collections of the Fairchild Tropical Botanic Garden (FTBG) in Coral Gables, FL. FTBG is located at 25.68°N/80.28°W, has a mean annual temperature of 24.1°C and an average total annual precipitation of 130 cm. We took advantage of the FTBG's diverse collection by selecting study plants that were mature individuals, had canopies that received direct sunlight for most of the day, were accessible from the ground and represented different families. We ultimately selected 21 species from 20 different families that exhibited a variety of growth habits (Table S1). We measured the parameters describing the relationship between temperature and carbon assimilation, and the three different metrics of heat tolerance on one individual per species.

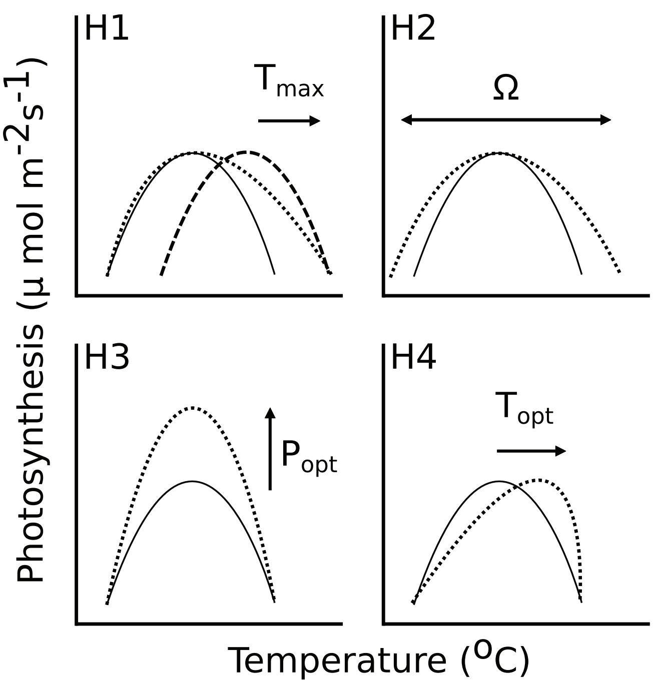

FIGURE 2 We address the assumption that PSII heat tolerance can promote greater carbon assimilation at higher temperature. Figure illustrates the change in a given trait between a species with a low heat tolerance (solid line) and high heat tolerance (dashed line). Hypothesis 1 (H1) proposes T_{max} is constrained by PSII heat tolerance, which could be associated with an increase in Ω (short dashed line), an increase in T_{max} (long dashed line), or a combination of the two; H2 is that high PSII heat tolerance promotes greater Ω indicative of a thermal generalist strategy of carbon assimilation; H3 that high PSII heat tolerance promotes higher P_{opt} characteristic of species with 'fast' carbon acquisition strategies and H4 that PSII heat tolerance promotes higher T_{opt}

2.2 | Temperature-assimilation curves

To estimate the carbon assimilation parameters used in this study (i.e. P_{opt}, T_{opt} T_{max} and Ω), we first repeatedly measured leaf temperature and net carbon assimilation for each of our study species using a LI-6800 portable photosynthesis system (LICOR, Lincoln, NE). More specifically, we randomly visited each focal plant during sunny days between 21 June and 1 September 2018, and measured carbon assimilation over a range of leaf temperatures within the canopy of each individual following the general methods of Slot and Winter (2017a). Leaf temperature was first measured on a set of randomly selected leaves within the canopy of each individual with an MT6 MiniTemp infrared thermometer (Raytek, Wilmington, NC). For each leaf, the LI-6800 cuvette was set to the observed temperature, and the leaf was allowed to acclimate to chamber conditions before its net assimilation was measured. During all measurements, the LI-6800 leaf chamber was maintained at saturating light levels (1,000 μmol quanta m^{-2} s^{-1}).

The CO_2 concentration was maintained at either 400 or 405 ppm in the reference chamber (differences due to operator error). Varying CO_2 reference chamber concentrations can potentially bias estimates of our carbon assimilation parameters. To correct for this, we conducted a separate set of measurements for 17 of our 21 species in which we varied the reference chamber CO_2 over a range of concentration to measure the effect that this could have on CO_2 assimilation in the sample chamber. We modelled this effect using the 'smooth. spline' function in base R's 'stats' package (Core, 2020) to calculate the difference in leaf assimilation rates between sample chamber CO_2 concentrations of 400 and 405 ppm. This difference was then added to assimilation measurements taken at 400 ppm to correct for any potential bias in our results. Even prior to correction, CO_2 concentrations within the sample chamber were uniformly distributed with a mean CO_2 concentration of 386 ppm and a *SD* of 8 ppm—a level of variation that is only slightly greater than those observed in leaf chambers of other studies (*SD* = 6 ppm; Slot & Winter, 2017a) and is unlikely to have affected our results.

The sample chamber's relative humidity was set to 50% during sampling but was automatically varied as needed to prevent moisture condensation within the LI-6800. In order to avoid measurement error, the LI-6800 reference and sample chambers' infrared gas analyzers were matched any time the sample chamber's leaf temperature was changed by ≥5°C since the previous match. We visually assessed stabilization of leaf temperatures, assimilation rates and stomatal conductances before recording carbon assimilation rate (μ mol m^{-2} s^{-1}).

Assimilation was modelled as a function of temperature following the model presented in June, Evans, and Farquhar (2004) and adapted by Slot and Winter (2017a):

$$P(T) = P_{opt} \times e^{-\left(\frac{T_{leaf} - T_{opt}}{\Omega}\right)^2}, \quad (1)$$

where T_{leaf} is leaf temperature and Ω is defined as the difference between the temperatures above and below T_{opt} at which assimilation (*P*) is reduced by ∼37% from P_{opt} (Figure 1a).

We estimated T_{max} and additional values of T_{opt} and P_{opt} following the model from Cunningham and Read (2003), which provides better fits for asymmetrical temperature-assimilation curves:

$$P = \left\{ b(T_{leaf} - T_{min}) \times \left[1 - e^{c(T_{leaf} - T_{max})}\right] \right\}^2, \quad (2)$$

where *b* and *c* are constants, *P* is the assimilation rate, T_{min} is the theoretical low-temperature compensation point and T_{max} is the theoretical high-temperature compensation point (Figure 1a).

The P_{opt}, T_{opt} and Ω parameters of Equation (1), and the *b*, *c*, T_{min} and T_{max} parameters from Equation (2) were estimated based on the fits of logistic non-linear least squares (nls) functions in R's base 'stats' package (Core, 2020). We bootstrapped the parameter estimates for each model and species by randomly resampling our leaf temperature and assimilation dataset 1,000 times with replacement. We present the bootstrapped means for P_{opt}, T_{opt} and Ω from Equation (1) and T_{max}, P_{opt} and T_{opt} from Equation (2).

2.3 | Determining T_{crit}, T_{50} and T_{95} heat tolerances

At the end of the study period, we collected random, fully expanded mature leaves from each focal individual and brought them to nearby laboratory facilities at the University of Miami. Depending on the size of the leaves, between 3 and 66 leaves were collected from each individual and used to determine the heat tolerances. Random leaflets from different leaves were sampled if species had compound leaves. Once in the lab, we used a hole punch to cut ∼1.9 cm diameter discs from the leaves. We placed six leaf discs from each individual in Miracloth fabric to prevent anaerobiosis during heat treatments (Krause et al., 2010); one layer of Miracloth was placed on the abaxial leaf surface, and three layers of Miracloth were placed on the adaxial leaf surface. We then placed the Miracloth-enclosed leaves into waterproof plastic bags with air removed and submerged in water baths maintained at room temperature (∼23°C), 38, 40, 42, 44, 46, 48, 50, 52, 54 or 60°C with circulating heaters. Immediately following 15-min of heat treatment, we removed the leaf pieces from water baths, placed them into petri dishes lined with moist paper towels and allowed them to recover for 24 hr at room temperature under low light (∼1 μmol photons m^{-2} s^{-1}). Following this recovery period, we dark-adapted the leaf pieces for 20 min before measuring their maximum quantum yield (F_v/F_m) with an OS30p+ handheld fluorometer (Opti-Science, Hudson, NH).

To estimate each species' T_{crit} and T_{50}, we modelled the relationship of F_v/F_m versus treatment temperature for each plant using the 'nls' function in base R's 'stats' package (Core, 2020). We calculated T_{crit} by finding the temperature where the slope of the F_v/F_m versus temperature relationship reached 15% of its most extreme value. We calculated T_{50} and T_{95} by predicting the temperature that caused a 50 or 95% reduction in F_v/F_m compared to the control treatment as:

$$heat\ tolerance = \frac{log\left(\frac{\theta_a}{x} - \theta_b\right)}{\theta_c}, \quad (3)$$

where θ_a is the asymptote of the heat treatment–response variable relationship, θ_b is a constant, *x* represents 50 or 95% reduction in F_v/F_m compared to control treatments and θ_c is the decay parameter. The θ parameters were fit to the temperature–response relationship using R's 'nls' function following:

$$y = \frac{\theta_a}{1 + e^{-(\theta_b + \theta_c T)}}, \quad (4)$$

where T is the heat treatment temperature (R Core Team, 2018). We generated bootstrapped means for T_{crit}, T_{50} and T_{95}, by randomly resampling data and fitting a new model for each species 100 times (Figure 1b). We present the mean bootstrapped values for T_{crit}, T_{50} and T_{95}.

2.4 | Data analysis

We generated a phylogenetic tree for our study species to help control for any potential phylogenetic non-independence in our dataset before testing our hypotheses H1-H4. We created a phylogeny from the trimmed R20120829 mega-tree (Gastauer & Meira-Neto, 2016) for our study species using the 'brranching' R package's 'phylomatic' function (Chamberlain, 2018). We assigned fossil-calibrated branch lengths for our tree using the ph_bladj function in the 'phylocomr' R package (Ooms & Chamberlain, 2018). Any polytomies were randomly resolved using the 'multi2di' function in the 'ape' R package (Paradis & Schliep, 2018).

We used our phylogenetic tree to compute a phylogenetic variance–covariance (VCV) matrix to test each of our four a priori hypotheses. Our VCV was calculated using the 'phytools' R package and its 'phyl.vcv' function (Revell, 2012). This approach assumes traits (in our case, the carbon assimilation and heat tolerance metrics) followed a Brownian model of evolution and that trait variance was proportional to branch lengths between two species and their most recent common ancestor. We divided the product of the inverse VCV and the observed trait values by the sum of the inverse VCV matrix to calculate the ancestral trait value at the root of our phylogeny (Blomberg, Garland, & Ives, 2003; Swenson, 2014). These root trait values were used to calculate a phylogenetically corrected covariation matrix among traits that was rescaled to compute Pearson's *r* using the 'cov2cor' function in R's base 'stats' package (R Core Team, 2020). The t-statistic and an α = .05 were used to test for significant trait correlations.

Below, we present the phylogenetically corrected correlations among traits as phylogenetically independent contrasts (PIC) for graphical purposes only. PICs were computed as the difference between two daughter nodes standardized by the square root of the sum of branch lengths (Felsenstein, 1985) and performed using the 'pic' function in the 'ape' R package (Paradis & Schliep, 2018) which results in $n - 1$ contrasts where 'n' is the number of species in the phylogeny. The correlations and PICs are calculated differently but provide effectively analogous results. We present only the statistics from the phylogenetically corrected correlations for simplicity in our figures. All analyses were conducted using R version 4.0.2 (Core, 2020).

3 | RESULTS

The final dataset that we used to model carbon assimilation as a function of temperature contained between 17 and 52 assimilation measurements per each of 21 plant species. Changes in the sample chamber concentrations from 400 to 405 ppm caused no more than a 0.27 μ mol m^{-2} s^{-1} increase in carbon assimilation (Figure S1). The fits of Equations (1) and (2) to our temperature-assimilation data are presented in Figure S2, and the carbon assimilation parameters (T_{max}, P_{opt}, T_{opt} and Ω) estimated from these models are provided in Table S1. The modelled changes in F_v/F_m in response to heat treatments used to calculate T_{crit}, T_{50} and T_{95} heat tolerances are presented in Figure S3 and provided in Table S1. Below, we present only values of T_{opt} and P_{opt} estimated using Equation (1) because they were highly correlated with their respective estimates from Equation (2). Results for hypotheses 3 and 4 using P_{opt} and T_{opt} from Equation (2) are provided in Figure S4.

We summarize the mean T_{opt}, T_{max}, T_{crit}, T_{50} and T_{95} relative to one another for each species and the entire dataset in Figure 3. The mean trait values for the entire dataset show that T_{max} is encompassed within the range of temperatures represented by the mean T_{crit} and T_{50}. This was not the case for species-level data as T_{crit} exceeded T_{max} for only seven species. T_{max} never exceeded T_{50}.

The only significant correlations we observed among carbon assimilation parameters involved the Ω parameter, which describes

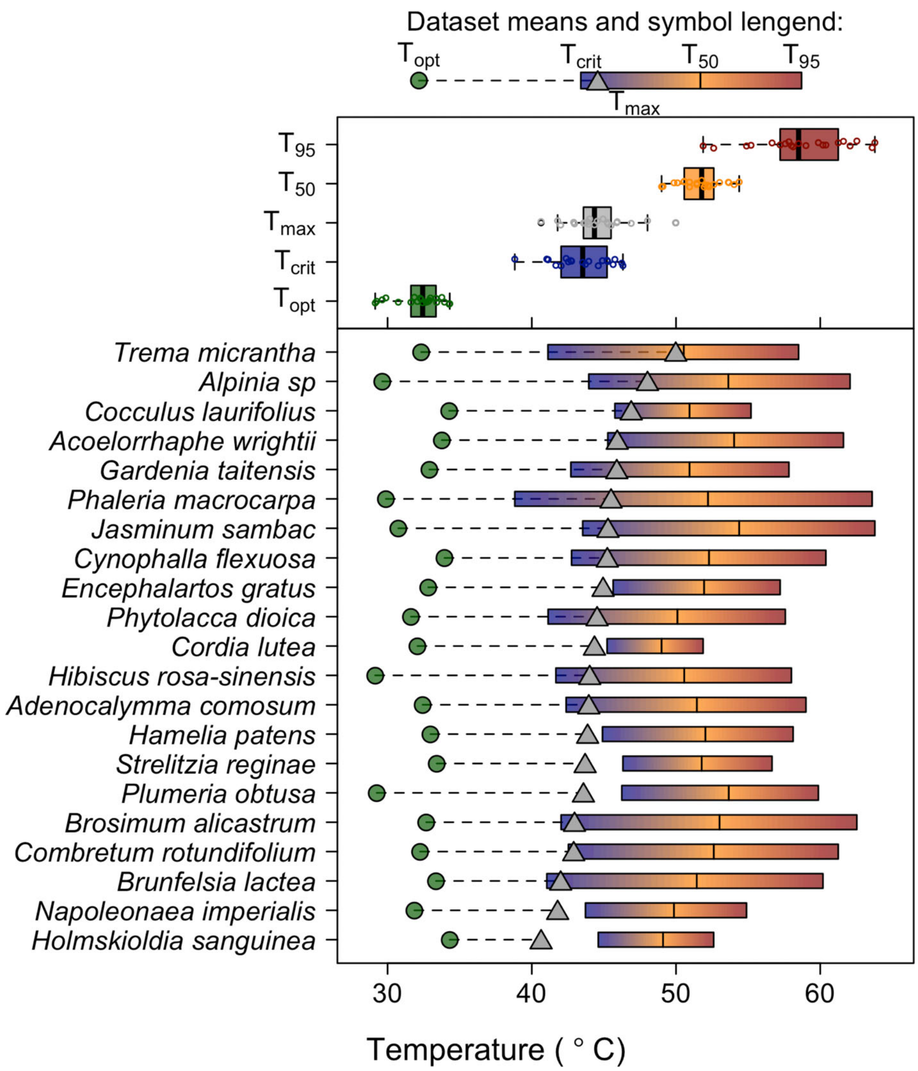

FIGURE 3 (top) The mean T_{opt} (circles), T_{crit} (left edge of the box), T_{max} (triangles), T_{50} (vertical line in centre of box) and T_{95} (right edge of box) for our dataset. The coloured boxes depict the thermal safety margins of PSII heat damage. Dotted lines connect the carbon assimilation traits; (middle) box plots of temperatures that correspond to the heat tolerance and carbon assimilation parameters of each species; (bottom) the relative temperatures of T_{opt}, T_{crit}, T_{max}, T_{50} and T_{95} for each species arranged from highest to lowest T_{max} [Colour figure can be viewed at wileyonlinelibrary.com]

the breadth of the temperature-assimilation curves. We observed that Ω was significantly correlated to T_{max} (r = 0.567, p = .007; Figure 4a), and negatively correlated to T_{opt} (r = 0.489, p = .024; Figure 4b). No

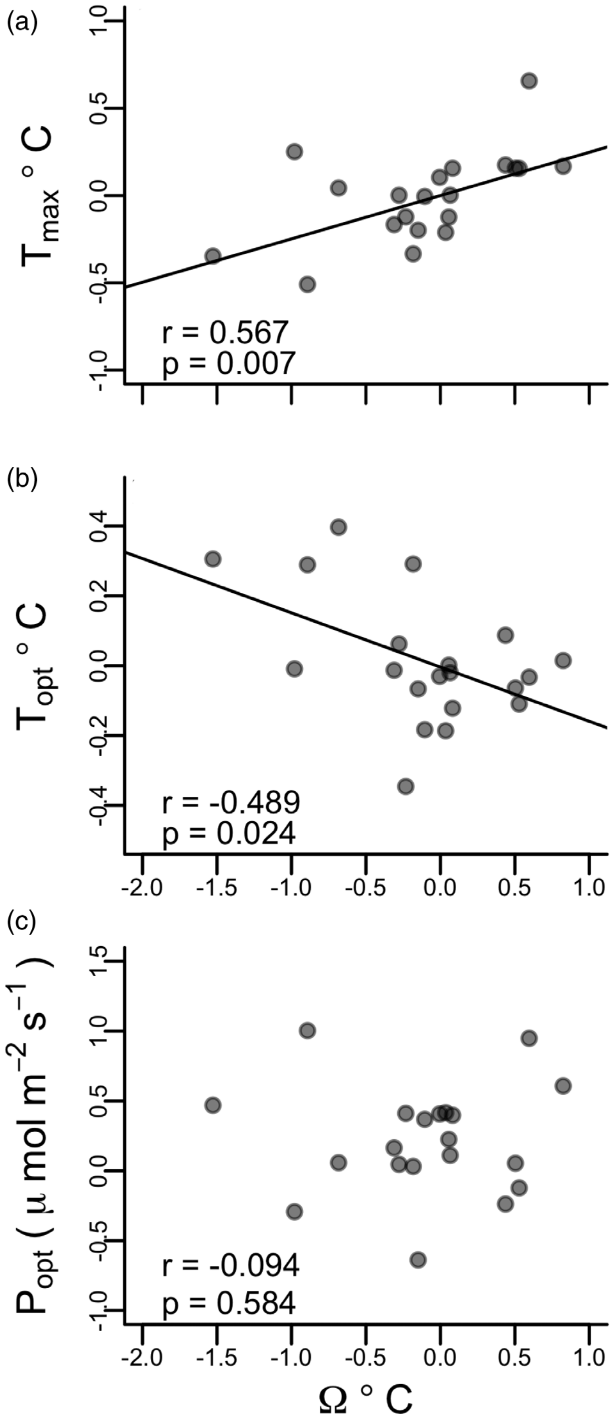

FIGURE 4 Here we illustrate the significant correlations among (a) Ω and T_{max}, (b) Ω and T_{opt} and (c) Ω and P_{opt} photosynthetic traits after correcting for phylogenetic independence. Each figure shows the phylogenetically independent contrasts for each trait with the phylogenetically corrected Pearson's correlation coefficient and significance in the bottom left corner. Solid lines within plots indicate significant correlations

correlations were observed between T_{opt} and P_{opt} estimated with either Equations (1) or (2) (Figure 4c).

The phylogenetically controlled correlations between different metrics of heat tolerance for PSII photochemistry and each parameter that describes carbon assimilation as a function of temperature are depicted in Figure 5. T_{crit} was negatively correlated to T_{95} (r = −0.486, p = .025) and not correlated to T_{50} (r = −0.089, p = .700). Our estimates of T_{50} and T_{95} were highly correlated (r = 0.91, p < .01) and exhibited similar relationships with the carbon assimilation parameters.

We found that T_{max} was not correlated with T_{crit}, T_{50} or T_{95} (Figure 5a–c; r = −0.334, p = .138; r = 0.270, p = .237; r = 0.372, p = .256), which does not support our hypothesis H1. T_{crit} was not correlated with Ω (Figure 5d; r = −0.190, p = .409), but in support of hypothesis H2, we found that T_{50} and T_{95} were positively correlated with Ω (Figure 5e,f; r = 0.581, p = .006; r = 0.590, p = .005). Our hypothesis H3 was not supported since we found that T_{crit} was not correlated with P_{opt} (Figure 5g; r = 0.211, p = .359), but T_{50} and T_{95} were negatively correlated with P_{opt} (Figure 5h,i; r = −0.495, p = .022; r = −0.521, p = .015). Similar results were obtained using assimilation estimates from Equation (2) (Figure S4A–C). Our hypothesis H4 was not supported as we observed no correlation between T_{crit} and T_{opt} from Equations (1) or (2) (Figure 5j; r = 0.193, p = .401; Figure S4D). Furthermore, we observed that T_{50} exhibited a marginally significant negative correlation to T_{opt} from Equation (1) (Figure 5k; r = −0.432, p = .051) and a significant negative correlation to T_{opt} from Equation (2) (Figure S4E). We found T_{95} that was negatively correlated to T_{opt} from Equation (1) (Figure 5l; r = −0.452, p = .039) but not from Equation (2) (Figure S4F). Two notable patterns among these relationships are that (a) correlations between T_{crit} and each carbon assimilation parameter were in the opposite direction as those observed for T_{50} and T_{95} and (b) heat tolerances that signify greater PSII impairment (i.e $T_{95} > T_{50} > T_{crit}$) tend to be more strongly correlated with carbon assimilation parameters, with the exception of T_{opt} from Equation (2) (Figure S4D–F).

When heat tolerances and carbon assimilation traits were not corrected for phylogenetic non-independence, the only significant correlation that persisted was between Ω and T_{opt}. Figure S2 suggests Equation (2) provided a poor fit for our *Hamelia patens* data. We excluded this species due to a potentially erroneous estimation of T_{max}, but exclusion of this species did not change our results, so it remained in our final results. We also log- and square root-transformed our estimates of T_{opt} and T_{crit}, respectively, to improve assumptions of normality before our phylogenetic corrections, but this had no effect on our results.

Given the poor coordination between T_{max} and our predefined estimates of PSII heat tolerance, we wanted to know if there was a predictable level of damage in F_v/F_m equal to T_{max}. We found that T_{max} is best characterized by a level of damage in PSII equivalent to the temperature that caused F_v/F_m to decrease by 7% (see Data S1). This heat tolerance was only correlated with T_{crit} (r = 0.70, p < .01) after performing the phylogenetic correction described above.

Decreases in assimilation above T_{opt} could be due to biochemical limitation at high temperatures or stomatal closure at high vapour pressure deficits (VPD). To better understand which was limiting

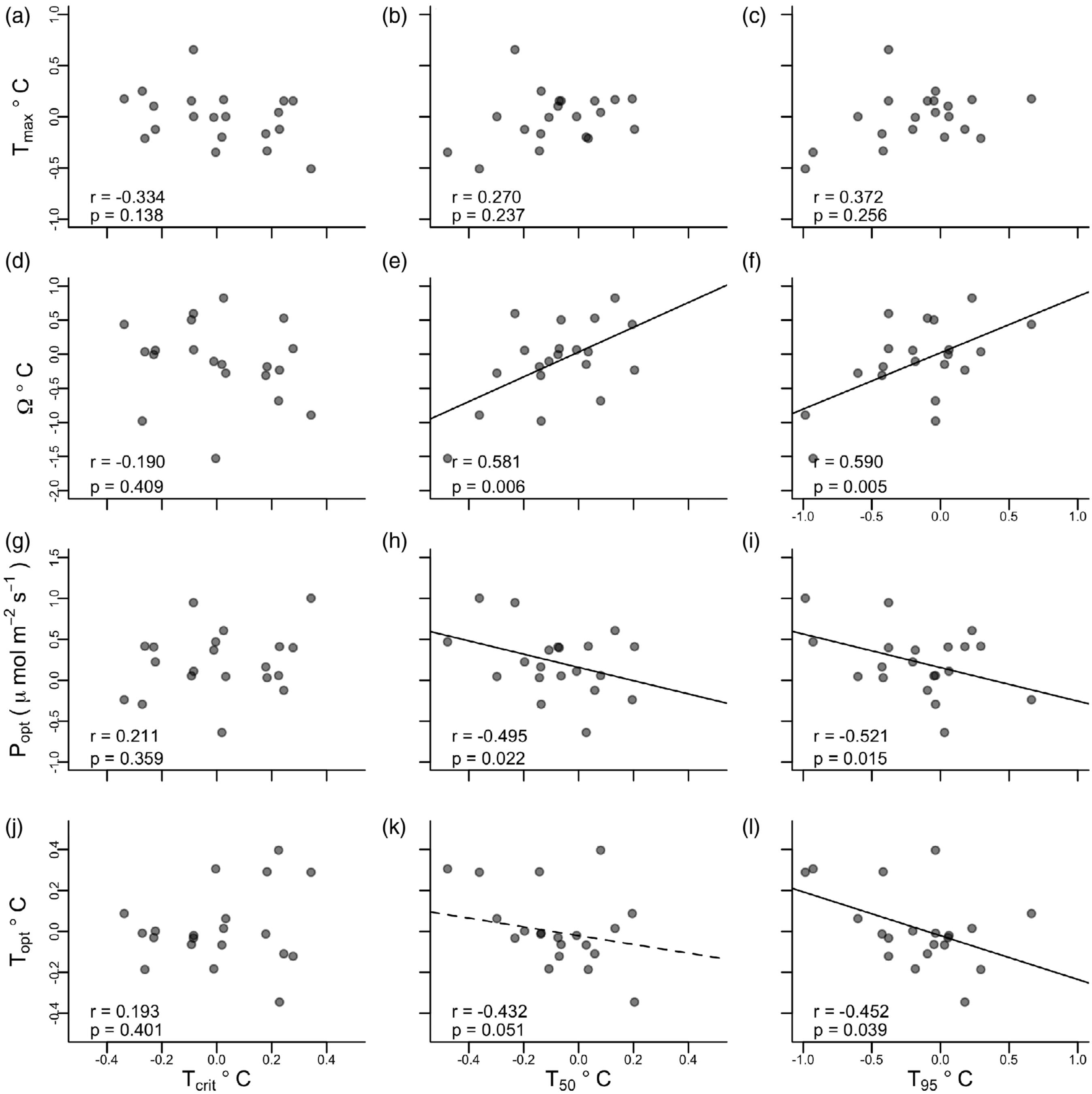

FIGURE 5 Here we illustrate the correlations among PSII heat tolerances and photosynthetic traits after correcting for phylogenetic independence. The top rows panels (a–c) correspond to hypothesis 1, panels (d–f) correspond to hypothesis 2; panels (g–i) correspond to hypothesis 3 and panels (j–l) correspond to hypothesis 4. Each figure shows the phylogenetically independent contrasts for each trait with the phylogenetically corrected Pearson's correlation coefficient and *p*-value in the bottom left corner. No line within a plot indicates no significant correlation, solid lines indicate significant correlations and the dashed line indicates a marginally significant correlation

carbon assimilation in our study, we tested the effect that leaf VPD and temperature had on stomatal conductance (g_s) and carbon assimilation at temperatures greater than T_{opt} (see Data S1). Although we were unable to effectively decouple the effects of VPD and temperature, the results of our linear mixed models suggest that leaf VPD is a stronger predictor of decreases in carbon assimilation and g_s than leaf temperature.

4 | DISCUSSION

We investigated the assumption that heat tolerances promote carbon assimilation at higher temperatures. We did not find support for our first hypothesis (H1) that PSII heat tolerance is coordinated with T_{max}. One reason that T_{max} may not be directly correlated with PSII heat tolerance is because both T_{max} and the T_{min} parameter used to fit

Equation (2) are purported to have no physiological significance (Cunningham & Read, 2003). It is also likely that stomatal closure ceases carbon assimilation before the actual thermal limits of plant biochemistry (i.e. electron transport or NADPH and ATP generation) are reached (Slot & Winter, 2017a, 2017b). While PSII heat tolerance and T_{max} were not correlated, we did find limited support for our hypothesis H1 that PSII heat tolerance provides a conservative high-temperature limit for T_{max}. Our estimates of T_{max} corresponded to the temperatures that caused between 0 and 45% damage to F_v/F_m, indicating that T_{50} may provide a reasonable upper bound for estimates of T_{max}. On the other hand, our estimates of T_{crit}, which corresponded to temperatures causing ~2% damage to F_v/F_m, were still higher than T_{max} for one third of our study species.

The positive correlations we observed between T_{50}, T_{95} and Ω support our second hypothesis (H2) that PSII heat tolerance is characteristic of thermal generalists. This is a notable result given that it is one of the only examples in plants providing an explicit physiological mechanism for the macroecological hypothesis that greater thermal variability should select for broader physiological tolerance (Janzen, 1967; Perez et al., 2016). Specifically, our results showed that species with the greatest thermal ranges for photosynthesis also tend to have the highest PSII heat tolerances. These results are also consistent with the predictions of leaf thermoregulatory theory.

Another prediction of the leaf thermoregulatory theory (Michaletz et al., 2015, 2016) is that P_{opt} may be positively correlated with high PSII heat tolerance (H3), but this is not supported by the negative correlations that we observed between T_{50}, T_{95} and P_{opt}. Instead, our results are consistent with the prediction that species with low carbon assimilation rates are likely to exhibit greater stress tolerance (Reich, 2014; Wright et al., 2004). Indeed, maintenance of PSII heat tolerance imposes a large metabolic cost that 'fast' species may not be able to support. PSII heat tolerance is linked to increased production of heat shock proteins (Wahid, Gelani, Ashraf, & Foolad, 2007), isoprenoids (Logan & Monson, 1999), photoprotective pigments (Krause et al., 2015), membrane-fortifying solutes (Hüve, Bichele, Tobias, & Niinemets, 2006) and the saturation of lipid bilayers (Zhu et al., 2018). The production of some of these metabolites may deplete the pools of NADPH and ATP that are available for carbon fixation as they are redirected to PSII thermoprotection (Gershenzon, 1994; Süss & Yordanov, 1986; Taylor, Smith, Slot, & Feeley, 2019; Voon & Lim, 2019; Wahid et al., 2007), explaining why P_{opt} decreases as PSII heat tolerance increases.

The high metabolic cost of PSII maintenance at high-temperature may also explain why heat tolerance was not positively correlated with T_{opt} in accordance with our fourth hypothesis (H4). Instead, our results suggested that high PSII heat tolerance may actually reduce T_{opt}. This counterintuitive relationship may be explained by the metabolic cost of maintaining high PSII heat tolerance described above. However, the negative relationship between heat tolerance, T_{opt} and P_{opt} may also be explained by stomatal closure.

High vapour pressure deficit can cause stomatal closure, which reduces carbon assimilation (Slot & Winter, 2017a, 2017b). When stomata close, latent heat loss is reduced and can lead to high leaf temperatures that are thought to drive variation in PSII heat tolerance (Perez & Feeley, 2020a). Therefore, if some plants possess inherently low stomatal conductance, it may explain why these species also tend to have low P_{opt} and high PSII heat tolerance. Indeed, our results indicate that carbon assimilation is more likely limited by high leaf VPD-induced stomatal closure than by the biochemical limits of photosynthesis like PSII photochemistry. This suggests that P_{opt} and T_{opt} have the potential to increase at higher leaf temperatures if VPD is alleviated (Varhammar et al., 2015), which could alter the relationships between carbon assimilation and PSII heat tolerances that we observed. This may offer some thermal resilience at higher concentrations of CO_2 (Smith et al., 2020), but tropical plants may still be in danger of approaching their biochemical limits of carbon assimilation under very high humidity that reduces VPD and latent heat loss (Perez & Feeley, 2018).

An important assumption we made was that our data were phylogenetically non-independent before we tested our hypotheses. Given that we measured species from a diverse set of families and clades (i.e. 21 species in 20 families), the topology and branch lengths of our phylogenetic tree are likely to provide a reasonable hypothesis of species relatedness. However, our assumption of phylogenetic non-independence could be violated if plasticity in PSII heat tolerance and carbon assimilation actually caused our trait estimates to be unrepresentative of each species (Sastry, Guha, & Barua, 2018; Way & Yamori, 2014). That said, our results currently suggest that there is strong covariation between some PSII heat tolerances and carbon assimilation parameters within phylogenies. Regardless of any phylogenetic correction, we confirmed that at the species-level, T_{max} occurs at lower temperatures than T_{50} but not T_{crit}, and that a community's mean T_{crit} may provide a reasonable approximation for T_{max}; however, we found little evidence to support the assumption that heat tolerance promotes carbon assimilation at high temperatures.

The protocols we followed to estimate heat tolerances prescribe a 24-hr recovery period before measuring the responses of F_v/F_m to the heat treatments. This 24-hr period recovery can cause estimates of heat tolerance to increase by up to 2°C compared to heat tolerances estimated using measurements of F_v/F_m taken immediately after heat treatment (Krause et al., 2010). To our knowledge, the capacity of F_v/F_m to recover among different species is poorly studied, which makes the effect of recovery time on our results unclear. Estimates of heat tolerances with smaller recovery times may provide better proxies for carbon assimilation and is an area for future research.

According to our phylogenetically corrected results, the only way that PSII heat tolerance may promote carbon assimilation at higher temperatures is by expanding Ω, but this benefit may be offset by concomitant decreases in T_{opt} and P_{opt}. This is potentially explained by high PSII heat tolerance promoting electron transport or the production of NADPH and ATP at high temperatures (Baker, 2008; Genty et al., 1989). We noted that the heat tolerances that signify greater PSII impairment (i.e. greater F_v/F_m damage) tended to have stronger correlations with carbon assimilation parameters. This is consistent with the hypothesis that larger reductions in the quantum yield have a greater effect on plant carbon economics, and may explain why T_{crit} heat tolerance was not correlated with any metric of carbon assimilation (Perez & Feeley, 2020a). Consequently, T_{95} may characterize plant thermal ecological strategies more effectively than T_{50} but provide overestimates of T_{max}.

Our results suggest that the heat tolerances of PSII measured with dark-adapted quantum yield (F_v/F_m) are not ideal proxies for carbon assimilation. Heat tolerances estimated with light-adapted quantum yield (F_q'/F_m') may be better proxies for assimilation (although these heat tolerance estimates are also subject to biases; Baker, 2008). Importantly, we show that T_{50} provides an upper bound for T_{max}. We also show that high PSII heat tolerance is characteristic of thermal generalist plant species with 'slow' carbon acquisition strategies. These results increase our understanding of the high-temperature limits of photosynthesis and can potentially be used to explain macroecological patterns in plant responses to climate change. More specifically, since PSII heat tolerance can characterize thermal specialization, it may prove useful for predicting the thermal specialists and generalists that are hypothesized to be most and least vulnerable to climate change, respectively (Perez & Feeley, 2020a).

ACKNOWLEDGMENTS

The authors would like to thank Fairchild Tropical Botanic Garden for providing access to their collections and two anonymous reviewers who provided constructive feedback on this manuscript. This research was conducted with the support of the Garden Club of America's Award in Tropical Botany to Timothy M. Perez and US National Science Foundation (NSF) DEB-1350125 to Kenneth J. Feeley.

CONFLICT OF INTEREST

The authors declare no conflicts of interest.

DATA AVAILABILITY STATEMENT

All data is available in Table S1.

ORCID

Timothy M. Perez https://orcid.org/0000-0002-3707-7285

REFERENCES

Baker, N. R. (2008). Chlorophyll fluorescence: A probe of photosynthesis in vivo. *Annual Review of Plant Biology*, *59*, 89–113.

Blomberg, S. P., Garland, T., & Ives, A. R. (2003). Testing for phylogenetic signal in comparative data: Behavioral traits are more labile. *Evolution*, *57*, 717–745.

Brooks, A., & Farquhar, G. D. (1985). Effect of temperature on the CO_2/O_2 specificity of ribulose-1,5-bisphosphate carboxylase/oxygenase and the rate of respiration in the light. *Planta*, *165*, 397–406.

Chamberlain S. (2018) brranching: Fetch "Phylogenies" from many sources.

Clark, D. A., Piper, S. C., Keeling, C. D., & Clark, D. B. (2003). Tropical rain forest tree growth and atmospheric carbon dynamics linked to interannual temperature variation during 1984–2000. *Proceedings of the National Academy of Sciences*, *100*, 5852–5857.

R Core Team (2020). *R: A language and environment for statistical computing*. Vienna, Austria: R Foundation for Statistical Computing.

Cunningham, S. C., & Read, J. (2003). Do temperate rainforest trees have a greater ability to acclimate to changing temperatures than tropical rainforest trees? *New Phytologist*, *157*, 55–64.

Doughty, C. E., & Goulden, M. L. (2009). Are tropical forests near a high temperature threshold? *Journal of Geophysical Research: Biogeosciences*, *114*, 1–12.

Downton, W. J. S., Berry, J. A., & Seemann, J. R. (1984). Tolerance of photosynthesis to high temperature in desert plants. *Plant Physiology*, *74*, 786–790.

Feeley, K., Martinez-villa, J., Perez, T., & Duque, A. S. (2020). The thermal tolerances, distributions, and performances of tropical montane tree species. *Frontiers in Forests and Global Change*, *3*, 1–11.

Feeley, K. J., Bravo-Avila, C., Fadrique, B., Perez, T. M., & Zuleta, D. (2020). Climate-driven changes in the composition of new world plant communities. *Nature Climate Change*, *10*, 965–970.

Felsenstein, J. (1985). Phylogenies and the comparative method. *The American Naturalist*, *125*, 1–15.

Gastauer, M., & Meira-Neto, J. A. A. (2016). An enhanced calibration of a recently released megatree for the analysis of phylogenetic diversity. *Brazilian Journal of Biology*, *76*, 619–628.

Genty, B., Briantais, J.-M., & Baker, N. R. (1989). The relationship between the quantum yield of photosynthetic electron transport and quenching of chlorophyll fluorescence. *Biochimica et Biophysica Acta (BBA) – General Subjects*, *990*, 87–92.

Gershenzon, J. (1994). Metabolic costs of terpenoid accumulation in higher plants. *Journal of Chemical Ecology*, *20*, 1281–1328.

Ghalambor, C. K., Huey, R. B., Martin, P. R., Tewksbury, J. J., & Wang, G. (2006). Are mountain passes higher in the tropics? Janzen's hypothesis revisited. *Integrative and Comparative Biology*, *46*, 5–17.

Huey, R. B. (2012). Predicting organismal vulnerability to climate warming: Roles of behaviour, physiology and adaptation. *Philosophical Transactions of the Royal Society B*, *367*, 1665–1679.

Huey, R. B., & Hertz, P. E. (1984). Is the jack of all trades a master of none? *Evolution*, *38*, 441–444.

Hüve, K., Bichele, I., Tobias, M., & Niinemets, Ü. (2006). Heat sensitivity of photosynthetic electron transport varies during the day due to changes in sugars and osmotic potential. *Plant, Cell and Environment*, *29*, 212–228.

Janzen, D. H. (1967). Why mountain passes are higher in the tropics. *The American Naturalist*, *101*, 233–249.

June, T., Evans, J. R., & Farquhar, G. D. (2004). A simple new equation for the reversible temperature dependence of photosynthetic electron transport: A study on soybean leaf. *Functional Plant Biology*, *31*, 275–283.

Krause, G. H., Winter, K., Krause, B., Jahns, P., García, M., Aranda, J., & Virgo, A. (2010). High-temperature tolerance of a tropical tree, Ficus insipida: Methodological reassessment and climate change considerations. *Functional Plant Biology*, *37*, 890.

Krause, G. H., Winter, K., Krause, B., & Virgo, A. (2015). Light-stimulated heat tolerance in leaves of two neotropical tree species, Ficus insipida and Calophyllum longifolium. *Functional Plant Biology*, *42*, 42–51.

Logan, B. A., & Monson, R. K. (1999). Thermotolerance of leaf discs from four isoprene-emitting species is not enhanced by exposure to exogenous isoprene. *Plant Physiology*, *120*, 821–826.

Mau, A., Reed, S., Wood, T., & Cavaleri, M. (2018). Temperate and tropical forest canopies are already functioning beyond their thermal thresholds for photosynthesis. *Forests*, *9*, 47.

Maxwell, K., & Johnson, G. N. (2000). Chlorophyll fluorescence – A practical guide. *Journal of Experimental Botany*, *51*, 659–668.

Michaletz, S. T., Weiser, M. D., Mcdowell, N. G., Zhou, J., Kaspari, M., Helliker, B. R., & Enquist, B. J. (2016). The energetic and carbon economic origins of leaf thermoregulation. *Nature Plants*, *2*, 1–8.

Michaletz, S. T., Weiser, M. D., Zhou, J., Kaspari, M., Helliker, B. R., & Enquist, B. J. (2015). Plant thermoregulation: Energetics, trait –

Environment interactions, and carbon economics. *Trends in Ecology & Evolution*, *30*, 1–11.

Ooms J. & Chamberlain S. (2018) phylocomr: Interface to "Phylocom"

Paradis E. & Schliep K. (2018) ape 5.0: An environment for modern phylogenetics and evolutionary analyses in R.

Pau, S., Detto, M., Kim, Y., & Still, C. J. (2018). Tropical forest temperature thresholds for gross primary productivity. *Ecosphere*, *9*, 1–12.

Perez, T. M., & Feeley, K. J. (2018). Increasing humidity threatens tropical forests. *Frontiers in Ecology and Evolution*, *6*, 1–2. https://doi.org/10.1071/FP10034

Perez, T. M., & Feeley, K. J. (2020a). Photosynthetic heat tolerances and extreme leaf temperatures. *Functional Ecology*, *34*, 2236–2245.

Perez, T. M., & Feeley, K. J. (2020b). Weak phylogenetic and climatic signals in plant heat tolerance. *Journal of Biogeography*. https://doi.org/10.1111/jbi.13984.

Perez, T. M., Stroud, J. T., & Feeley, K. J. (2016). Thermal trouble in the tropics. *Science*, *351*, 1392–1393.

Perez, T. M., Valverde-Barrantes, O., Bravo, C., Taylor, T. C., Fadrique, B., Hogan, J. A., … Feeley, K. J. (2019). Botanic gardens are an untapped resource for studying the functional ecology of tropical plants. *Philosophical Transactions of the Royal Society of London. Series B, Biological Sciences*, *374*, 1–9.

R Core Team (2018). *version 3.4.4. R: A language and environment for statistical computing*. Vienna, Austria: R Foundation for Statistical Computing. https://www.R-project.org/.

Reich, P. B. (2014). The world-wide "fast-slow" plant economics spectrum: A traits manifesto. *Journal of Ecology*, *102*, 275–301.

Revell, L. J. (2012). Phytools: An R package for phylogenetic comparative biology (and other things). *Methods in Ecology and Evolution*, *3*, 217–223.

Sastry, A., Guha, A., & Barua, D. (2018). Leaf thermotolerance in dry tropical forest tree species: Relationships with leaf traits and effects of drought. *Annals of Botany*, *10*, 1–13.

Seemann, J. R., Berry, J. A., & Downton, W. J. S. (1984). Photosynthetic response and adaptation to high temperature in desert plants: A comparison of gas exchange and fluorescence methods for studies of thermal tolerance. *Plant Physiology*, *75*, 364–368.

Slot, M., Krause, G. H., Krause, B., Hernández, G. G., & Winter, K. (2018). Photosynthetic heat tolerance of shade and sun leaves of three tropical tree species. *Photosynthesis Research*, *141*, 119–130.

Slot, M., & Winter, K. (2017a). In situ temperature response of photosynthesis of 42 tree and liana species in the canopy of two Panamanian lowland tropical forests with contrasting rainfall regimes. *New Phytologist*, *214*, 1103–1117.

Slot, M., & Winter, K. (2017b). In situ temperature relationships of biochemical and stomatal controls of photosynthesis in four lowland tropical tree species. *Plant Cell and Environment*, *40*, 3055–3068.

Smith, M. N., Taylor, T. C., Van, H. J., Rosolem, R., Restrepo-coupe, N., Adams, J., … Saleska, S. R. (2020). Empirical evidence for resilience of tropical forest photosynthesis in a warmer world. *Nature Plants*, *6*, 1225–1230.

Süss, K. H., & Yordanov, I. T. (1986). Biosynthetic cause of in vivo acquired thermotolerance of photosynthetic light reactions and metabolic responses of chloroplasts to heat stress. *Plant Physiology*, *81*(1), 192–199.

Swenson, N. G. (2014). In R. Gentleman, K. Hornik, & G. Permigiani (Eds.), *Functional and phylogenetic ecology in R*. New York, NY: Springer.

Taylor, T. C., Smith, M. N., Slot, M., & Feeley, K. J. (2019). The capacity to emit isoprene differentiates the photosynthetic temperature responses of tropical plant species. *Plant, Cell & Environment*, *42*, 2448–2457.

Tiwari, R., Gloor, E., Jonatar, W., Cruz, A., Marimon, B. S., Marimon-junior, B. H., … Vitória, A. P. (2020). Photosynthetic quantum efficiency in south-eastern Amazonian trees may be already affected by climate change. *Plant Cell and Environment*, 1–12. https://doi.org/10.1111/pce.13770

Valladares, F., & Pearcy, R. W. (1997). Interactions between water stress, sun-shade acclimation, heat tolerance and photoinhibition in the sclerophyll *Heteromeles arbutifolia*. *Plant, Cell & Environment*, *20*, 25–36.

Varhammar, A., Mclean, C. M., Dusenge, M. E., Medlyn, B. E., Hasper, T. B., Nsabimana, D., & Uddling, J. (2015). Photosynthetic temperature responses of tree species in Rwanda: Evidence of pronounced negative effects of high temperature in montane rainforest climax species. *New Phytologist*, *206*, 1000–1012.

Voon, C. P., & Lim, B. L. (2019). ATP translocation and chloroplast biology. *National Science Review*, *6*, 1073–1076. https://doi.org/10.1093/nsr/nwz089

Wahid, A., Gelani, S., Ashraf, M., & Foolad, M. (2007). Heat tolerance in plants: An overview. *Environmental and Experimental Botany*, *61*, 199–223.

Way, D. A., & Yamori, W. (2014). Thermal acclimation of photosynthesis: On the importance of adjusting our definitions and accounting for thermal acclimation of respiration. *Photosynthesis Research*, *119*, 89–100.

Wright, I. J., Reich, P. B., Westoby, M., Ackerly, D. D., Baruch, Z., Bongers, F., … Gulias, J. (2004). The worldwide leaf economics spectrum. *Nature*, *428*, 821–827.

Zhu, L., Bloomfield, K. J., Hocart, C. H., Egerton, J. J. G., O'Sullivan, O. S., Penillard, A., … Atkin, O. K. (2018). Plasticity of photosynthetic heat tolerance in plants adapted to thermally contrasting biomes. *Plant Cell and Environment*, *41*, 1251–1262.

SUPPORTING INFORMATION

Additional supporting information may be found online in the Supporting Information section at the end of this article.

How to cite this article: Perez TM, Socha A, Tserej O, Feeley KJ. Photosystem II heat tolerances characterize thermal generalists and the upper limit of carbon assimilation. *Plant Cell Environ*. 2021;1–10. https://doi.org/10.1111/pce.13990